Published in final edited form as:
*Mol Carcinog*. 2014 September ; 53(9): 722–735. doi:10.1002/mc.22024.

# Growth Inhibition of Pancreatic Cancer Cells by Histone Deacetylase Inhibitor Belinostat Through Suppression of Multiple Pathways Including HIF, NFkB, and mTOR Signaling In Vitro and In Vivo

**Wenwen Chien**[1,*], **Dhong Hyun Lee**[2], **Yun Zheng**[2,3], **Peer Wuensche**[1], **Rosie Alvarez**[2], **Ding Ling Wen**[1], **Ahmed M. Aribi**[2], **Su Ming Thean**[1], **Ngan B. Doan**[4], **Jonathan W. Said**[4], and **H. Phillip Koeffler**[1,2,5]

[1]Cancer Science Institute of Singapore, National University of Singapore, Singapore, Singapore

[2]Division of Hematology and Oncology, Cedars-Sinai Medical Center, Los Angeles, California

[3]Department of Hepatobiliary Oncology, State Key Laboratory of Oncology in South China, Cancer Center, Sun Yat-sen University, Guangzhou, Guangdong, P. R. China

[4]Department of Pathology and Laboratory Medicine, UCLA School of Medicine, Los Angeles, California

[5]National University Cancer Institute, Singapore, Singapore

## Abstract

Pancreatic ductal adenocarcinoma is a devastating disease with few therapeutic options. Histone deacetylase inhibitors are a novel therapeutic approach to cancer treatment; and two new pan-histone deacetylase inhibitors (HDACi), belinostat and panobinostat, are undergoing clinical trials for advanced hematologic malignancies, non-small cell lung cancers and advanced ovarian epithelial cancers. We found that belinostat and panobinostat potently inhibited, in a dose-dependent manner, the growth of six (AsPc1, BxPc3, Panc0327, Panc0403, Panc1005, MiaPaCa2) of 14 human pancreatic cancer cell lines. Belinostat increased the percentage of apoptotic pancreatic cancer cells and caused prominent $G_2$/M growth arrest of most pancreatic cancer cells. Belinostat prominently inhibited PI3K-mTOR-4EBP1 signaling with a 50% suppression of phorphorylated 4EBP1 (AsPc1, BxPc3, Panc0327, Panc1005 cells). Surprisingly, belinostat profoundly blocked hypoxia signaling including the suppression of hypoxia response element reporter activity; as well as an approximately 10-fold decreased transcriptional expression of VEGF, adrenomedullin, and HIF1α at 1% compared to 20% $O_2$. Treatment with this HDACi decreased levels of thioredoxin mRNA associated with increased levels of its endogenous inhibitor thioredoxin binding protein-2. Also, belinostat alone and synergistically with gemcitabine significantly ($P = 0.0044$) decreased the size of human pancreatic tumors grown in immunodeficiency mice. Taken together, HDACi decreases growth, increases apoptosis, and is



[*]Correspondence to: Cancer Science Institute of Singapore, National University of Singapore, 14 Medical Drive, #12-01, Singapore 117599, Singapore.
Wenwen Chien and Dhong Hyun Tony Lee contributed equally to this work.

associated with blocking the AKT/mTOR pathway. Surprisingly, it blocked hypoxic growth related signals. Our studies of belinostat suggest it may be an effective drug for the treatment of pancreatic cancers when used in combination with other drugs such as gemcitabine.

### Keywords

4EBP1; hypoxia; thioredoxin; panobinostat

## INTRODUCTION

Over 250 000 individuals are diagnosed annually worldwide with pancreatic ductal adenocarcinoma (PDAC) [1]. In 2010, about 43 000 new cases and 36 800 deaths occurred from pancreatic malignancy in the United States [2]. PDAC has a high mortality rate in part because it is typically only diagnosed at an advanced refractory stage when surgery can no longer entirely remove the tumor. Radiation therapy and/or currently used chemotherapy, gemcitabine (2′,2′–difluorodeoxycytidine) a deoxycytidine analog, are palliative at best [3]. Although small molecule kinase inhibitors have been developed, their therapeutic efficacy for pancreatic cancer is limited [4,5]. Over 90% of pancreatic cancers have a mis-sense mutation of K-RAS and constitutive activation of multiple downstream pathways including the RAF-mitogen-activated kinase (MAPK) and phosphoinositide-3-kinase (PI3K) circuits [6,7]. About half of the tumors have p53, SMAD4, and/or p15/p16/ARF mutations, but they also have 60–120 additional genomic changes that vary between each of the cancers [8,9].

Inhibitors for histone deacetylases (HDACi) have provided a promising new approach in cancer therapy and are currently in several clinical trials [10]. These HDACi enhance the transcription of target genes by acetylating histones in region of the gene which increases the accessibility of chromatin [11,12]. In addition, many proteins become acetylated by HDACis and their activities altered [11,13]. Taken together, these HDACis have a myriad of effects confounding our ability to ascribe an anti-cancer activity to one mode of action. Butyrate is one of the earliest HDACi directed against class I HDAC [14]; it sensitizes FAS-mediated apoptosis and synergizes with gemcitabine against PDAC in vitro [15]. Pan-HDACi such as vorinostat (SAHA) and trichostatin causes a G2/M–phase arrest and p21 up-regulation in PDAC in vitro [16]. In pancreatic cancer xenotransplant models, TSA synergizes with gemcitabine, and SAHA synergizes with bortezomib [17,18]. In our study, the antiproliferative activity of two new pan-HDACi (belinostat and panobinostat) was examined using a panel of 14 human pancreatic cancer cell lines. Belinostat and panobinostat suppressed cell proliferation of these human pancreatic cancer cells. Further studies focusing on belinostat showed that it caused growth arrest and apoptosis. The drug inhibited both the PI3K-mTOR-p4EBP, nuclear factor-kappaB (NFkB), as well as the hypoxia-inducible factors (HIF) signaling pathways. Also, Belinostat inhibited human pancreatic cancer cell growth and worked synergistically with gemcitabine to inhibit pancreatic cancer cell growth in immunodeficient mice. In summary, belinostat is associated with growth inhibition in pancreatic cancer cells and may provide clinical benefit for patients with this devastatingly, rapidly fatal disease.

## MATERIALS AND METHODS

### Cell Lines

Pancreatic cancer cell lines (AsPc1 BxPc3, Panc1, Panc0203, Panc0327, Panc0403, Panc0504, Panc0813, Panc1005, CFPAC1, CaPan2, MiaPaCa2, PL45, SU8686) were purchased from the American Type Culture Collection (Manassas, VA) and cultured in either DMEM or RPMI-1640 supplemented with 10% FBS.

### Statistical Analysis

All statistical analysis was performed using Graph-Pad Prism (Graphpad, La Jolla, CA). *P*-values < 0.05 were statistically significant and were designated with "*" in figures.

### MTT Assays

Five thousand cells per well were seeded in 96-well plates overnight followed by treatment for 48 h with different concentrations of drugs. For combination treatment, both drugs were simultaneously added together in the culture medium. Growth inhibition was assayed by MTT (3-(4,5-Dimethylthiazol-2-yl)-2,5-diphenyltetrazolium bromide). Results were calculated from three independent experiments with quadruplicates each time. EC50 was calculated using GraphPad Prism software and Sigmoidal Model.

### Drugs

Belinostat was kindly provided by National Cancer Institute/National Institute of Health for animal studies. Belinostat and panobinostat were also purchased from Selleck (Houston, TX). SAHA was from LC Laboratories (Woburn, MA). Each was prepared as a 10 mM stock in DMSO for MTT assays and belinostat was prepared in diluent (100 mg/mL L-arginine in water) for animal studies. For in vivo drug combination, the two drugs were simultaneously added to the diluents and immediately injected into the peritoneal cavity of mice.

### Cell Cycle and Apoptosis Analyses

Cells were seeded in 6-well plates at subconfluent density and were treated with drugs for 24–48 h. Cells were harvested, fixed with 70% ethanol, and stained with propidium iodide solution (10 μg/mL) with RNase A (200 μg/mL). Cell cycle analysis was performed using BD LSRII flow cytometer (BD Biosciences, San Jose, CA) and ModFit LT cell cycle analysis software. For apoptosis assay after drug treatment, cells were harvested and assayed using Annexin V apoptosis detection kit (BD Pharmingen, San Jose, CA). Results are representative of three independent experiments after analyzed with FlowJo software (Tree Star, Ashland, OR).

### Western Blot Analysis

Cell lysates were prepared with lysis buffer containing 1% NP40, 0.1% SDS in 50 mM Tris–HCl (pH 7.5) with cocktail protease inhibitors. Thirty microgram of protein lysates were subjected to SDS-polyacrylamide gel electrophoresis followed by Western blot analysis. Antibodies were purchased from Cell Signaling and Santa Cruz. Chemiluminescent

substrate West Dura (Thermo Scientific, Rock-ford, IL) was used for detection of protein of interest. Results were representative of three independent experiments.

### Real-Time Reverse Transcription PCR

RNA was harvested from cell lines using Qiagen RNase kit (Qiagen, Hilden, Germany) according to the manufacturer's instructions, followed by DNase treatment to remove genomic DNA. Two microgram of RNA was reverse transcribed with first strand cDNA synthesis kit (Fermentas, Vilnius, Lithuania). Real-time PCR was performed with SYBR Green reagents (Fermenta) in triplicates in Applied Biosystems 7500 Fast PCR system. PCR products were checked for specificity on a 2% agarose gel. Messenger RNA expression levels were normalized to levels of GAPDH, and relative target gene expression was determined. Results were calculated from two independent experiments with triplicates each time.

### Reporter Assays

Cells were plated at subconfluent density and transfected with 1 μg of the reporter plasmid and internal control of 25 ng *renilla* luciferase pRL-TK. The HRE-LUC and NFkB-LUC each contains three repeats of the hypoxia response element and the NF kappa B binding site, respectively, upstream of thymidine kinase minimal promoter in front of the luciferase cDNA (a generous gift of Dr. Lorenz Poellinger, Cancer Science Institute Singapore, National University of Singapore). After transfection, cells were treated with 1 μM of belinostat for 24 h. Dual Luciferase Assay Kit (Promega) was used for detection of reporter activation. Data were calculated and presented as fold increase after normalized to *renilla* activity. Results were derived from triplicates of two independent experiments.

### Animal Studies

BxPc3 pancreatic cancer cells ($5 \times 10^6$) were subcutaneously injected into both flanks of mice. Drug injections were started when the tumor became palpable (day 3). For the combination studies, the drugs were prepared simultaneously together in the diluents. All injections were given three times a week. The last drug administration was on day 35 and tumor was harvested on day 38. Tumor size was compared between treatment with combination of belinostat and gemcitabine and single agent. Tumors were harvested and weighed. Protein lysates were prepared for Western blot analysis and paraffin-fixed tumors for immunohistochemical analysis (IHC) of phospho-4EBP1 and phospho-p70S6K. Four groups of drug treatments included: (1) 30 mg/kg belinostat, (2) 30 mg/kg belinostat plus 15 mg/kg gemcitabine, (3) 15 mg/kg gemcitabine, and (4) diluent (100 mg/mL L-arginine in water). One-way ANOVA including Bartlett's test for equal variances and Kolmogorov–Smirnov for normality was used to determine significant difference ($P < 0.05$) among four different treatment groups. In vivo experiments were repeated once. For IHC, slides from tumor xenograft tissue were prepared as previously described [19]. 293T cells overexpressing eukaryotic translation initiation factor 4E-binding protein 1 (4EBP1), LC3, and p70S6k were used as positive controls and empty vector transfected 293T cells were used as negative control for antibodies. Antibodies of 1:100 dilutions of antibodies were used. Representative microscopic fields are shown in 200-fold magnification. Analysis for

toxic side effects included complete blood counts and serum chemistries were performed as previously reported [19] using Hemagen Analyst® Benchtop Chemistrym System (Hemagen Diagnostic, MD).

## RESULTS

### Belinostat and Panobinostat: Histone Deacetylase Inhibitors Suppressed Cell Proliferation of Pancreatic Cancer Cells In Vitro

In order to determine the sensitivity of pancreatic cancer cells to the antiproliferative activity of belinostat and panobinostat (HDACi), we examined their effects on a large panel of 14 human pancreatic cancer cell lines. The $EC_{50}$ for each cell line was calculated after testing with a series of concentrations of the two HDACi after a relatively short 48 h exposure. Potency of the two HDACi as measured by curves of growth inhibition showed nearly parallel decrease in cell viability albeit at a different scale. Six cell lines (AsPc1, BxPc3, Panc0327, Panc0403, Panc1005, MiaPaCa2) were very sensitive to belinostat ($EC_{50}$: ranged between 0.3 and 1.1 μM) (Figure 1A). Among these six, three cell lines (Panc0327, MiaPaCa2, Panc0403) were sensitive to panobinostat with an $EC_{50}$ ranging between 0.5 and 13 nM and two (BxPc3, Panc1005) were moderately sensitive to panobinostat at the 300 nM range (Figure 1C). For the eight cell lines (PL45, Panc0203, Panc1, SU8686, Panc0813, CaPan2, CFPAC) that were either only modestly sensitive or resistant to belinostat (Figure 1B), each was also resistant to panobinostat (Figure 1D). $EC_{50}$ of these pancreatic cancer cell lines were listed in Figure 1F. Belinostat-sensitive cell lines were treated with the FDA-approved HDACi SAHA to compare drug potency. MTT results for five cell lines (BxPc3, Panc0327, Panc0403, Panc1005, MiaPaCa2) showed that belinostat and SAHA had comparable cell killing abilities; and belinostat had greater growth inhibitory potency than SAHA for three pancreatic cancer cell lines (Panc0327, Panc0403, MiaPaCa2; Figure 1D).

### Belinostat Induced Apoptosis and Growth Arrest, As Well As Autophagy in Pancreatic Cancer Cell Lines

Cell cycle analysis was performed on belinostat-treated pancreatic cancer cells to examine the mechanisms of the antiproliferative activity of the drug. Of the six cell lines, three (Panc0327, Panc1005, Panc0403) showed increase in cell apoptosis (pre-$G_0$; Figure 2A). Two cell lines (AsPc1, MiaPaCa2) had an elevation in the $G_2$/M fraction of cells, and one cell line (BxPc3) displayed an increase in the $G_0/G_1$ fraction. The apoptosis and growth arrest were dose-dependent, as an increase in belinostat from 1 to 10 μM increased both the percentage of apoptotic Panc0403 cells (from 23% to 39%, respectively), and the percentage of cells that were growth arrested in $G_2$/M in AsPc1 (40–47%) and MiaPaCa2 (46–53%, respectively; Figure 2B).

Real-time quantitative RT-PCR and Western analysis examined expression levels of cell cycle-regulated, apoptosis-, and autophagy-related transcripts and proteins. Real-time RT-PCR of two cell lines (Panc0327, Panc1005) showed that belinonstat treatment markedly increased expression (6- to 14-fold) of the pro-apoptotic cyclin-dependent kinase inhibitor p21 and death receptor 5 (DR5; Figure 3A). Western blot analysis of a panel of pancreatic cancer cell lines demonstrated that p21 protein levels were correspondingly increased in

belinostat-treated pancreatic cancer cells, while protein expression levels of the anti-apoptotic protein Bcl-xL decreased (Figure 3B). In addition, real-time PCR showed that belinostat profoundly decreased levels of the cell-growth related cyclin D1, CDK2, CDK4, and TNFα (Figure 3C), but also induced the expression levels of the autophagy marker LC3 (Figure 3D). Additionally, the TNFα-stimulated NFκb reporter activity was suppressed after the cells (AsPc1, BxPc3, Panc0327, Panc1005) were treated with belinostat (Figure 3E).

## Belinonstat Inhibited Signaling by the PI3K-mTOR-4EBP1 and HIF Pathways

As expected, increase in acetylation of histone 3 was observed in belinonstat-treated pancreatic cancer cells as shown by Western blot analysis (Figure 4A). Basal phosphorylation level of the downstream target of mammalian target of rapamycin (mTOR), translational repressor protein 4EBP1 was decreased after belinostat treatment (Figure 4A). Serum-starved pancreatic cancer cells stimulated with epidermal growth factor (EGF), ligand for EGF receptor, activated the Erk and p70S6K pathways. Belinostat blocked this EGF-mediated kinase activation, blocking these two downstream targets (Figure 4B). Next, we examined if belinostat had a direct effect on EGFR. After serum-starvation overnight, EGFR activation by EGF was suppressed by pre-treatment with belinostat. In addition to decreased EGFR phosphorylation, expression of EGFR was also decreased (Figure 4C).

Pancreatic cancers typically grow within hypoxic conditions; therefore, a hypoxia response element reporter assay was used to examine the effect of belinostat on HIF activation. Belinonstat treatment (1 μM, 24 h) inhibited the HRE reporter activity in four pancreatic cancer cell lines (AsPc1, BxPc3, Panc0327, Panc1005; Figure 5A). In pancreatic cancer cells (Panc0327, Panc1005), the inhibition of HIF transcriptional activity was associated with decreased expression levels of HIF1α and VEGF, as well as, hypoxia-inducible protein, adrenomedullin (ADM; Figure 5B). A previous study showed that SAHA-induced expression of thioredoxin binding protein-2 (also known as either vitamin D3 upregulated protein 1 or thioredoxin interacting protein [TXNIP]) was associated with a decrease in thioredoxin (TXN) in prostate cancer. TXN is involved in HIF1α stabilization and VEGF expression. We found that belinostat treatment of pancreatic cancer cells increased expression of the TXNIP and decreased levels of TXN (Figure 5C).

## Pancreatic Cancer Cell Growth Was Synergistically Inhibited by Belinostat and Gemcitabine In Vitro and in an Animal Model With Low Toxicity

We first evaluated potential synergism between belinostat and the FDA-approved therapeutic drug gemcitabine in vitro. Cell death by gemcitabine (5 μg/mL) treatment of belinostat-sensitive human pancreatic cancer cell line BxPc3 was synergistic in vitro when combined with belinostat at 1 μM (Figure 6A). We explored this potential synergy in additional cell lines including both belinostat-sensitive and -resistant ones. Among five sensitive cell lines, two (Panc0403, Panc0203) showed synergism between belinostat and gemcitabine; and among six resistant cell lines, the combination was synergistic in five cell lines (Panc0504, CFPAC, CaPanc2, Panc0813, Panc1; Figure 6B). To identify the mechanism of synergy in both the belinostat-sensitive and -resistant cell lines, Western blot analysis was performed to detect autophagy-related molecules (ATG5, LC3) and phosphorylated p70s6k. Belinostat by itself, induced expression of ATG5, LC3, and

suppressed p70s6k phosphorylation in the sensitive cell lines (Figure 6C, left panel). In the resistant cell lines, belinostat had minimal effect on either ATG5 or LC3 levels, but suppressed p70s6k phosphorylation levels (Figure 6C, right panel). Gemcitabine alone did not induce LC3 in either sensitive or resistant cell lines (Figure 6D). Cells treated with belinostat together with gemcitabine did not exhibit additional increase in LC3 expression, but did show slightly additional decrease in expression levels of anti-apoptotic Bcl-xL in both belinostat-sensitive and –resistant cell lines (Figure 6D). We accessed this synergism against human pancreatic cancer xenografts (BxPc3 cells). BxPC3 is a model of poorly differentiated pancreatic adenocarcinoma. The growth of the tumors was inhibited by belinostat treatment, and the combination of belinostat with gemcitabine showed synergistic ($P = 0.0152$) anti-proliferative effects. When tumors were harvested on day 38, the mean (±SD) tumor weight of belinostat-treated mice was 302 ± 103 g, and those who received the drug combination had tumors with a mean (±SD) weight of 136 ± 14 g (Figure 7A). Dissected tumors at completion of the trial were examined by both Western blot and immunohistochemistry analysis. Tumors from mice treated with either belinonstat or the combination of belinonstat and gemcitabine showed decreased expression of phosphorylated 4EBP1 compared to tumors from diluent-treated mice by Western blot analysis (Figure 7B). Also, tumors of gemcitabine treated mice had increased expression of LC3 in both the cytoplasm (LC3-I) and autophagosome (LC3-II; Figure 7B). Tumors from belinostat treated mice showed only the active form of LC3-II (Figure 7B). Combination of belinonstat and gemcitabine displayed a dramatic increase in the activation of LC3-II (Figure 7B). Immunohistochemistry analysis with phosphorylated 4EBP antibody showed decreased staining in tissue treated with the combination of gemcitabine and belinostat (Figure 7C). Staining for LC3 antibody was negative in control tissue and the staining was increased in the drug combination treated tissue (Figure 7C).

Toxic side-effects of belinostat were evaluated. Body weight of mice showed no significant change when comparing the four groups (Table 1). The weights of the kidneys and livers were also not significantly different. Mild enlargement of spleen was observed in mice which received gemcitabine as either a single agent or combined with belinostat (Table 2). No significant changes were found in the white blood cell and platelet counts. Significant reduction in the hemoglobin levels occurred only in the gemcitabine and the combination groups, suggesting gemcitabine caused anemia in the mice (Table 3). Evaluation of a panel of 16 serum chemistry parameters showed no significant changes (Table 4).

## DISCUSSION

The family of HDACi has become potential therapeutic agents for solid tumors and lymphoid hematological malignancies [10]; indeed SAHA (vorinostat) has been approved for treatment of advanced primary cutaneous T-cell lymphomas [20]. Currently, several new HDACis are undergoing clinical studies including belinostat and panobinostat, which are in trials for advanced hematopoietic, non-small cell lung, and advanced ovarian epithelial cancers [21–23]. In this study, we showed that belinostat and panobinostat are potent inhibitors of proliferation of human pancreatic cancer cells. Proliferation assays determined the EC50 for belinostat was within the micromolar range and panobinostat was in the nanomolar range when tested against a panel of 14 human pancreatic cancer cell lines. The

different scales of effective concentrations of these two HDACis suggest in-depth toxicity studies are necessary to address potential host toxicities in their clinical use. Our murine studies showed no obvious toxicities of belinostat at a therapeutic concentration. Our data demonstrated that belinostat showed greater growth inhibitory potency than SAHA against three pancreatic cancer cell lines (Panc0327, Panc0403, MiaPaCa2).

In various cancer models, HDACis induced cell death, as well as inhibited tumor growth and angiogenesis [24–26]. Studies to explain the mechanism of actions of these HDACis have not provided a clearly unified answer, but the effective target of the drug may vary depending on the cellular context of the tumor cells [27,28]. Immunoblot analysis of four cell lines (AsPc1, BxPc3, Panc0327, Panc1005) demonstrated that belinostat increased histone acetylation and thereby opened the chromatin structure, allowing enhanced gene transcription. Also, four of the six examined lines had growth arrest associated with either accumulation at either the G0/G1 or G2/M phase of the cell cycle after exposure to belinostat. Apoptosis was observed only in Panc0327 and Panc0504 cells after belinostat treatment. Quantitative real-time RT-PCR and immunoblot analysis for proteins involved in regulation of the cell cycle and apoptosis suggested that the HDACi modulated p21, cyclin D1, CDK2, CDK4, DR5, and Bcl-xL. In the future, comparison of the genetic profiles of pancreatic cancer cells may facilitate predicting which tumors will be responsive to therapy with belinostat.

Previous studies showed that the HDACi SAHA and butyrate induced programmed cell death and caspase-independent autophagic cell death [29] and SAHA induced p21 activity and enhanced cell death by gemcitabine in pancreatic cancer cells [30]. Panobinostat has been shown to potentiate TRAIL-induced apoptosis by cFLIP degradation [31]. Our results from real-time qPCR demonstrated induction of autophagy marker LC3 and Western analysis showed increase expression of LC3 and another autophagy-related molecule ATG5. We also observed these pancreatic cancer cells treated with belinostat exhibited features of autophagic cell death such as rounded cell shapes and appearance of abundance of cytoplasmic vacuoles (data not shown). Western blot analysis of tumors from our animal studies also showed activation of autophagy and combined treatment with belinostat and gemcitabine induced abundant expression of lipidated LC3-II. In pancreatic cancer cells, belinostat is likely to elicit autophagy, apoptosis, and cell growth arrest.

Previous studies suggested that blockade of the NFκB pathway was required to enhance HDACi-mediated lethality of leukemia and head and neck squamous carcinoma cells [32]. The rationale was that acetylation of RelA/p65 by HDACi promoted nuclear accumulation and activation of NFκB. However, our results showed that belinostat suppressed the anti-proliferative TNFα-stimulated NFκB reporter activity in pancreatic cancer cell lines. Our data suggest that the activity of belinostat against pancreatic cancer cells may be mediated through other components of the NFκB pathway in addition to either RelA/p65 or crosstalk between NFκB pathway and other signaling pathways.

Nearly 100% of pancreatic adenocarcinomas have a K-RAS mutation. Activated K-RAS promotes the PI3K signaling pathway, and the serine/threonine kinase mTOR is activated [33]. Our results showed EGF-mediated activation of EGFR, Erk, and p70s6k was

suppressed in pancreatic cancer cells treated with belinostat, most likely through the loss of EGFR expression. The mTOR pathway regulates cell proliferation by phosphorylating p70 ribosomal S6 kinase (p70S6k) and 4EBP1. We previously showed that SAHA could inhibit this pathway in B cell lymphoma cells [34]. Also, the benzamide MS-275 HDACi blocks Akt/mTOR signaling in acute myeloid leukemia cells (HL60, NB4) [35]. We showed that belinostat treatment of belinostat-sensitive pancreatic cancer cells suppressed cell proliferation associated with decreased expression of proteins required for initiation of translation. Our study is the first to our knowledge to show that the HDACi belinostat suppressed mTOR signaling through dephosphorylation of p70S6k and 4EBP1 in pancreatic cancer cells.

Hypoxia is a key regulatory factor in tumor progression [36]; and in response to hypoxic stress, the HIFs are the primary responsive transcriptional factors [37]. In the presence of hypoxia, HIFs regulate cell metabolism and redox homeostasis [38]. In our study, belinostat treatment of pancreatic cancer cells suppressed levels of HIF1α and its target genes VEGF and ADM. ADM is overexpressed in various malignant tumors such as glioblastomas, breast cancers, and pancreatic adenocarcinomas [39–41]. In pancreatic cancer cells, ADM is inducible by hypoxia and glucose deprivation. Expression of ADM in pancreatic cancer cells stimulats cell proliferation and enhances cell invasion [41]. Small interfering RNA targeting ADM increased tubulin acetylation, reduced cell motility, and caused growth arrest in the G2 phase [42]. ADM has been suggested to be a potential therapeutic target. Our data suggest the effect of belinostat on HIF signaling is associated with suppression of pancreatic cancer cell growth.

In addition, treatment with belinostat also induced the expression of the TXN inhibitor TXNIP. TXN is regulated by thioredoxin reductase and NADPH in response to oxidative stress. TXN is able to up-regulate VEGF and angiogensis; and in a variety of tumors, TXN is elevated [40,43]. Chemicals targeting TXN have been developed as potential anti-cancer therapy [44]. A previous study showed that expression of TXNIP was induced by direct binding of SAHA to the TXNIP promoter region [45]. We found that belinostat treatment increased transcriptional levels of TXNIP. Thus, similar to SAHA, belinostat may induce expression of TXNIP by interacting with its promoter, resulting in decreased TXN activity.

Our in vitro combination studies in six belinostat-sensitive and six-resistant cell lines demonstrated that the synergy between gemcitabine and belinostat was not cell line specific. In belinostat-senstivie cells we identified that autophagy-related molecules ATG5 and LC3, as well as anti-apoptotic Bcl-xL were involved in the mechanisms underlying synergy between gemcitabine and belinonstat. In comparison to belinostat-sensitive cells, exposure of the resistant cell lines to belinostat had nearly the same effect on the suppression of activities of p70s6k and Bcl-xL, but no effect on expression levels of autophagy- and HIF-related molecules. These data suggest that synergism between belinostat and gemcitabine in belinostat-resistant cells may be different from sensitive cells. Although belinostat-sensitive cell line BxPc3 was used in in vivo studies, our in vitro results from belinostat-resistant cell lines suggested the combination of belinostat and gemcitabine would suppress belinostat-resistant pancreatic tumor growth in vivo. Additionally, targeting autophagy and HIF signaling has the potential to initiate death of these resistant cells.

In this study, we showed that pancreatic cancer cells were susceptible to belinostat both in vitro and in vivo. Belinostat efficiently suppressed the growth of the human pancreatic cancer xenografts placed in nude mice. Although the chosen dosage of gemcitabine in our study showed minimum effects on the growth of xenograft, the combination of belinostat with gemcitabine synergistically suppressed the tumor growth. Immunohistochemistry and Western blot analysis of tumors demonstrated the growth suppression produced by belinostat was associated with decrease in the phosphorylation levels of 4EBP1, a critical protein involved in translation regulation [46]. Immunoblots also showed the induction of lipidated LC3 and suggested the formation of cellular autophagosomes and activation of autophagy [47]. No significant toxic side-effects were observed in mice treated with belinostat, and a minor decrease of red cells was found in mice treated with either gemcitabine or the combination of gemcitabine plus belinostat. No significant change occurred in white blood cell populations and platelets.

In summary, our in vitro studies demonstrated that belinostat suppressed pancreatic cancer cell growth by at least three pathways: mTOR, NFkB and HIF. Belinonstat affected the regulation of protein synthesis and cell proliferation. A xenograft murine model assay further demonstrated the in vivo efficacy of belinostat in pancreatic cancer. Belinostat may have potential therapeutic efficacy for the treatment of pancreatic cancers.

## Acknowledgments

We especially thank Marcia and Jeff Green for their generous support for pancreatic cancer research.

## Abbreviations

| | |
|---|---|
| **NFkB** | nuclear factor-kappaB |
| **HIF** | hypoxia-inducible factors |
| **4EBP1** | eukaryotic translation initiation factor 4E-binding protein 1 |
| **mTOR** | mammalian target of rapamycin |

## References

1. Vincent A, Herman J, Schulick R, Hruban RH, Goggins M. Pancreatic cancer. Lancet. 2011; 378:607–620. [PubMed: 21620466]
2. Jenks S. AACR highlights: Promise for treating pancreatic cancer. J Natl Cancer Inst. 2011; 103:766–767.
3. Colucci G, Labianca R, Di Costanzo F, et al. Randomized phase III trial of gemcitabine plus cisplatin compared with single-agent gemcitabine as first-line treatment of patients with advanced pancreatic cancer: The GIP-1 study. J Clin Oncol. 2010; 28:1645–1651. [PubMed: 20194854]
4. Adachi Y, Yamamoto H, Ohashi H, et al. A candidate targeting molecule of insulin-like growth factor- I receptor for gastrointestinal cancers. World J Gastroenterol. 2010; 16:5779–5789. [PubMed: 21154998]
5. Kim LC, Song LX, Haura EB. Src kinases as therapeutic targets for cancer. Nat Rev Clin Oncol. 2009; 6:587–595. [PubMed: 19787002]
6. Janku F, Lee JJ, Tsimberidou AM, et al. PIK3CA mutations frequently coexist with RAS and BRAF mutations in patients with advanced cancers. PLoS ONE. 2011; 6:e22769. [PubMed: 21829508]
7. McCarthy N. Pancreatic cancer on your marks. Nat Rev Cancer. 2009; 9:846.

8. Campbell PJ, Yachida S, Mudie LJ, et al. The patterns and dynamics of genomic instability in metastatic pancreatic cancer. Nature. 2010; 467:1109–1113. [PubMed: 20981101]
9. Dong XQ, Jiao L, Li YA, et al. Significant associations of mismatch repair gene polymorphisms with clinical outcome of pancreatic cancer. J Clin Oncol. 2009; 27:1592–1599. [PubMed: 19237629]
10. Prince HM, Bishton MJ, Harrison SJ. Clinical studies of histone deacetylase inhibitors. Clin Cancer Res. 2009; 15:3958–3969. [PubMed: 19509172]
11. Marks PA, Richon VM, Rifkind RA. Histone deacetylase inhibitors: Inducers of differentiation or apoptosis of transformed cells. J Natl Cancer Inst. 2000; 92:1210–1216. [PubMed: 10922406]
12. Johnstone RW, Licht JD. Histone deacetylase inhibitors in cancer therapy: Is transcription the primary target? Cancer Cell. 2003; 4:13–18. [PubMed: 12892709]
13. Li Y, Kao GD, Garcia BA, et al. A novel histone deacetylase pathway regulates mitosis by modulating Aurora B kinase activity. Genes Dev. 2006; 20:2566–2579. [PubMed: 16980585]
14. Candido EPM, Reeves R, Davie JR. Sodium butyrate inhibits histone deacetylation in cultured-cells. Cell. 1978; 14:105–113. [PubMed: 667927]
15. Natoni F, Diolordi L, Santoni C, Montani MSG. Sodium butyrate sensitises human pancreatic cancer cells to both the intrinsic and the extrinsic apoptotic pathways. Biochim Biophys Acta-Mol Cell Res. 2005; 1745:318–329.
16. Kumagai T, Wakimoto N, Yin D, et al. Histone deacetylase inhibitor, suberoylanilide hydroxamic acid (Vorinostat, SAHA) profoundly inhibits the growth of human pancreatic cancer cells. Int J Cancer. 2007; 121:656–665. [PubMed: 17417771]
17. Carew JS, Medina EC, Esquivel JA, et al. Autophagy inhibition enhances vorinostat-induced apoptosis via ubiquitinated protein accumulation. J Cell Mol Med. 2010; 14:2448–2459. [PubMed: 19583815]
18. Gahr S, Ocker M, Ganslmayer M, et al. The combination of the histone-deacetylase inhibitor trichostatin A and gemcitabine induces inhibition of proliferation and increased apoptosis in pancreatic carcinoma cells. Int J Oncol. 2007; 31:567–576. [PubMed: 17671683]
19. Lee DH, Thoennissen NH, Goff C, et al. Synergistic effect of low-dose cucurbitacin B and low-dose methotrexate for treatment of human osteosarcoma. Cancer Lett. 2011; 306:161–170. [PubMed: 21440986]
20. Kavanaugh SA, White LA, Kolesar JM. Vorinostat: A novel therapy for the treatment of cutaneous T-cell lymphoma. Am J Health-Syst Pharm. 2010; 67:793–797. [PubMed: 20479100]
21. Lassen U, Molife LR, Sorensen M, et al. A phase I study of the safety and pharmacokinetics of the histone deacetylase inhibitor belinostat administered in combination with carboplatin and/or paclitaxel in patients with solid tumours. Br J Cancer. 2010; 103:12–17. [PubMed: 20588278]
22. Mackay HJ, Hirte H, Colgan T, et al. Phase II trial of the histone deacetylase inhibitor belinostat in women with platinum resistant epithelial ovarian cancer and micropapillary (LMP) ovarian tumours. Eur J Cancer. 2010; 46:1573–1579. [PubMed: 20304628]
23. Gimsing P, Hansen M, Knudsen LM, et al. A phase I clinical trial of the histone deacetylase inhibitor belinostat in patients with advanced hematological neoplasia. Eur J Haematol. 2008; 81:170–176. [PubMed: 18510700]
24. Wedel S, Hudak L, Seibel JM, et al. Critical analysis of simultaneous blockage of histone deacetylase and multiple receptor tyrosine kinase in the treatment of prostate cancer. Prostate. 2011; 71:722–735. [PubMed: 20954195]
25. Lee KH, Choi EY, Kim MK, et al. Inhibition of histone deacetylase activity down-regulates urokinase plasminogen activator and matrix metalloproteinase-9 expression in gastric cancer. Mol Cell Biochem. 2010; 343:163–171. [PubMed: 20559690]
26. Shimura H, Furuya F, Aoyagi M, Ohta K, Endo T, Kobayashi T. A proteosome inhibitor synergizes with histone deacetylase inhibitor-induced cell death and redifferentiation of thyroid carcinoma cells. Endocr J. 2010; 57:S463.
27. Huang XP, Gao LZ, Wang SL, Lee CK, Ordentlich P, Liu BL. HDAC inhibitor SNDX-275 induces apoptosis in erbB2-over-expressing breast cancer cells via down-regulation of erbB3 expression. Cancer Res. 2009; 69:8403–8411. [PubMed: 19826038]

28. Park JH, Kim SH, Choi MC, et al. Class II histone deacetylases play pivotal roles in heat shock protein 90-mediated proteasomal degradation of vascular endothelial growth factor receptors. Biochem Biophys Res Commun. 2008; 368:318–322. [PubMed: 18211808]
29. Park MA, Zhang G, Martin AP, et al. Vorinostat and sorafenib increase ER stress, autophagy and apoptosis via ceramide-dependent CD95 and PERK activation. Cancer Biol Ther. 2008; 7:1648–1662. [PubMed: 18787411]
30. Arnold NB, Arkus N, Gunn J, Korc M. The histone deacetylase inhibitor suberoylanilide hydroxamic acid induces growth inhibition and enhances gemcitabine-induced cell death in pancreatic cancer. Clin Cancer Res. 2007; 13:18–26. [PubMed: 17200334]
31. Kauh J, Fan S, Xia M, et al. c-FLIP degradation mediates sensitization of pancreatic cancer cells to TRAIL-induced apoptosis by the histone deacetylase inhibitor LBH589. PLoS ONE. 2010; 5:e10376. [PubMed: 20442774]
32. Duan JM, Friedman J, Nottingham L, Chen Z, Ara G, Van Waes C. Nuclear factor-kappa B p65 small interfering RNA or proteasome inhibitor bortezomib sensitizes head and neck squamous cell carcinomas to classic histone deacetylase inhibitors and novel histone deacetylase inhibitor PXD101. Mol Cancer Ther. 2007; 6:37–50. [PubMed: 17237265]
33. Bianco RB, Melisi D, Ciardiello F, Tortora G. Key cancer cell signal transduction pathways as therapeutic targets. Eur J Cancer. 2006; 42:290–294. [PubMed: 16376541]
34. Kawamata N, Chen J, Koeffler HP. Suberoylanilide hydroxamic acid (SAHA; vorinostat) suppresses translation of cyclin D1 in mantle cell lymphoma cells. Blood. 2007; 110:2667–2673. [PubMed: 17606765]
35. Nishioka C, Ikezoe T, Yang J, Takeuchi S, Koeffler HP, Yokoyama A. MS-275, a novel histone deacetylase inhibitor with selectivity against HDAC1, induces degradation of FLT3 via inhibition of chaperone function of heat shock protein 90 in AML cells. Leuk Res. 2008; 32:1382–1392. [PubMed: 18394702]
36. Wilson WR, Hay MP. Targeting hypoxia in cancer therapy. Nat Rev Cancer. 2011; 11:393–410. [PubMed: 21606941]
37. Guillemin K, Krasnow MA. The hypoxic response: Huffing and HIFing. Cell. 1997; 89:9–12. [PubMed: 9094708]
38. Cannito S, Novo E, Compagnone A, et al. Redox mechanisms switch on hypoxia-dependent epithelial-mesenchymal transition in cancer cells. Carcinogenesis. 2008; 29:2267–2278. [PubMed: 18791199]
39. Ouafik L, Sauze S, Boudouresque F, et al. Neutralization of adrenomedullin inhibits the growth of human glioblastoma cell lines in vitro and suppresses tumor xenograft growth in vivo. Am J Pathol. 2002; 160:1279–1292. [PubMed: 11943713]
40. Martinez A, Vos M, Guedez L, et al. The effects of adrenomedullin overexpression in breast tumor cells. J Natl Cancer Inst. 2002; 94:1226–1237. [PubMed: 12189226]
41. Keleg S, Kayed H, Jiang XH, et al. Adrenomedullin is induced by hypoxia and enhances pancreatic cancer cell invasion. Int J Cancer. 2007; 121:21–32. [PubMed: 17290391]
42. Sackett DL, Ozbun L, Zudaire E, et al. Intracellular proadrenomedullin-derived peptides decorate the microtubules and contribute to cytoskeleton function. Endocrinology. 2008; 149:2888–2898. [PubMed: 18325988]
43. Welsh SJ, Bellamy WT, Briehl MA, Powis G. The redox protein thioredoxin-1 (Trx-1) increases hypoxia-inducible factor 1 alpha protein expression: Trx-1 overexpression results in increased vascular endothelial growth factor production and enhanced tumor angiogenesis. Cancer Res. 2002; 62:5089–5095. [PubMed: 12208766]
44. Wang XF, Zhang JS, Xu TW. Thioredoxin reductase inactivation as a pivotal mechanism of ifosfamide in cancer therapy. Eur J Pharmacol. 2008; 579:66–73. [PubMed: 18028906]
45. Butler LM, Zhou XB, Xu WS, et al. The histone deacetylase inhibitor SAHA arrests cancer cell growth, up-regulates thioredoxin-binding protein-2, and down-regulates thioredoxin. Proc Natl Acad Sci USA. 2002; 99:11700–11705. [PubMed: 12189205]
46. Shamji AF, Nghiem P, Schreiber SL. Integration of growth factor and nutrient signaling: Implications for cancer biology. Mol Cell. 2003; 12:271–280. [PubMed: 14536067]

47. Tanida I, Ueno T, Kominami E. LC3 conjugation system in mammalian autophagy. Int J Biochem Cell Biol. 2004; 36:2503–2518. [PubMed: 15325588]

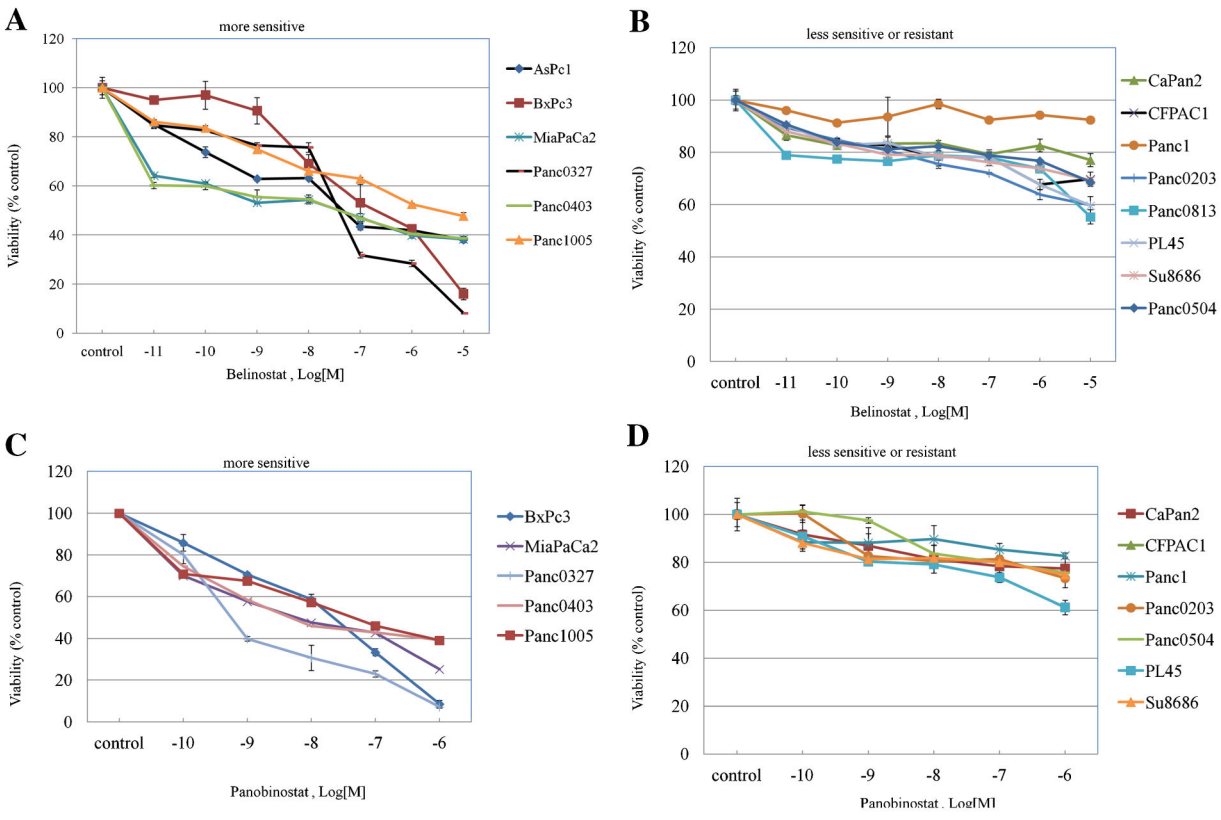


**E**

EC50 of pancreatic cancer cell lines after 48h exposure to either belinostat or panobinostat

| | Bel (μM)[a] | Pan (nM)[b] |
|---|---|---|
| AsPc1 | 0.3 | N.T. |
| Panc0327 | 0.5 | 0.46 |
| MiaPaCa2 | 0.7 | 13 |
| BxPc3 | 1.0 | 284 |
| Panc0403 | 1.1 | 7.7 |
| Panc1005 | 1.1 | 261 |
| PL45 | 20.8 | R |
| Panc0203 | 22.2 | R |
| Panc0504 | R | R |
| CFPAC1 | R | R |
| Su8686 | R | R |
| CaPan2 | R | R |
| Panc0813 | R | N.T. |
| Panc1 | R | R |

EC50: Concentration to achieve 50% cell death; Bel: Belinostat; Pan: Panobinostat; R: Resistant; [a]: R>50 μ M; [b]: R> 1 μM; N.T.: not tested;

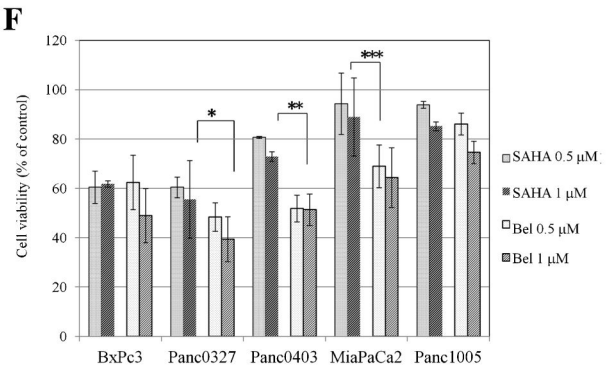


**Figure 1.**

Anti-proliferative activity of belinostat and panobinostat against 14 pancreatic cancer cell lines. Panels (A–D): MTT assays of pancreatic cancer cells cultured in 96-well plates and treated with drugs for 48 h. Cell numbers were measured after drug treatment relative to diluent controls. A series of dilutions ($1 \times 10^{-11}$ M to $1 \times 10^{-5}$ M) of belinostat (Panels A,B) or panobinostat (Panels C,D) were used. Panel (E): List of EC50s for belinostat and panobinostat against a panel of pancreatic cancer cell lines. Panel (F): Comparison between the anti-proliferative activity of belinostat and SAHA. Five pancreatic cancer cell lines were exposed to belinostat (0.5, 1 μM) or SAHA (0.5, 1 μM) for 48 h and MTT assays were performed. (*$P$ = 0.07; **$P$ = 0.013; ***$P$ = 0.03). Results represent the mean ± SD of three

independent experiments with quadruplicates at each time. Bel, belinostat; SAHA, veronistat.

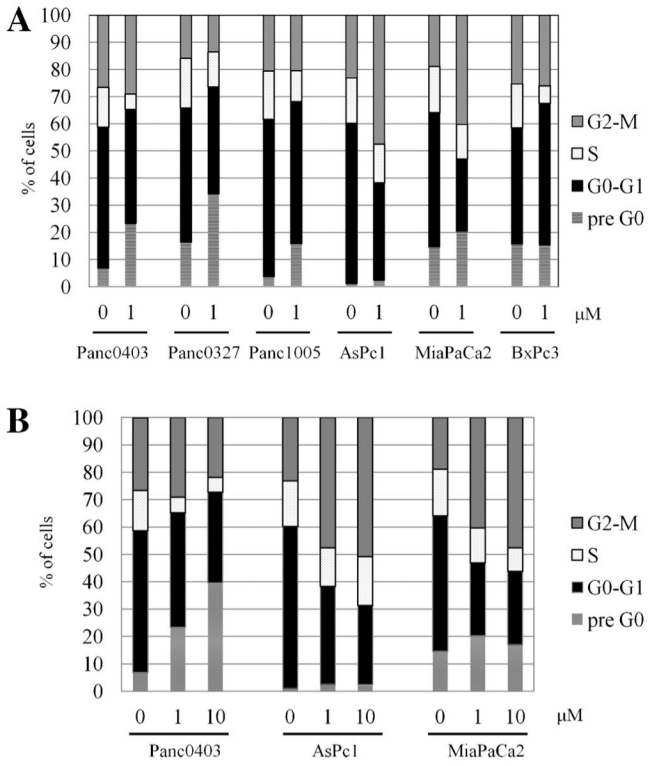


**Figure 2.**

Cell cycle analysis of pancreatic cancer cell lines treated with belinostat. Fluorescent activated cell sorter was used to analyze the cells stained with propidium iodide. Panel (A): Cell cycle analysis of six cell lines (AsPc1, BxPc3, MiaPaCa2, Panc0327, Panc0403, Panc1005) treated with belinostat (1 μM) for 24 h. Panel (B): Cell cycle analysis of three cell lines (AsPc1, MiaPaCa2, Panc0403) after 24 h treatment with diluent control (0), 1 and 10 μM belinostat. Results represent the mean ± SD of three independent experiments.

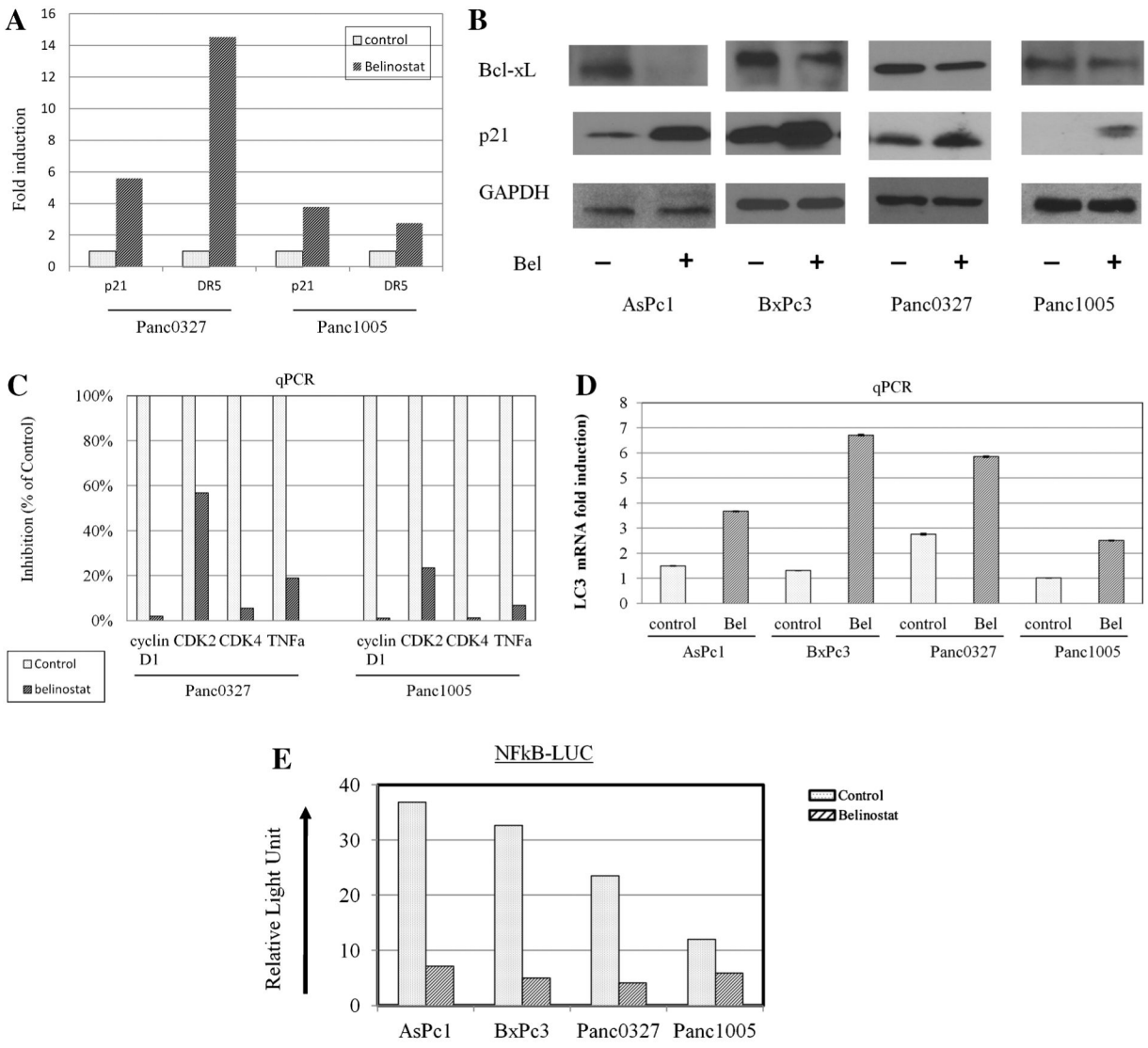


**Figure 3.**

Regulation by belinostat of genes involved in cell growth and apoptosis. Pancreatic cancer cell lines were treated with belinostat (1 μM, 24 h), and RNA and protein lysates were extracted for analysis. Panel (A): Real-time quantitative RT-PCR for transcriptional expression levels of p21 and DR5. Fold expression was normalized to GAPDH expression levels of the cells. Panel (B): Western blot analysis for protein expression of Bcl-xL and p21. GAPDH was used as loading control. Panel (C): Real-time quantitative RT-PCR for cyclin D1, CDK2, CDK4, and TNFα; expression levels were normalized to GAPDH. Panel (D): Real-time quantitative RT-PCR for LC3; expression levels were normalized to GAPDH. Panel (E): NFkB reporter assays. Cells were transfected with reporter construct and *renilla*, and incubated for 24 h. Thereafter, cells were exposed to belinostat for 8 h and treated with TNFα for 16 h. NFkB reporter activity was normalized to *renilla* activity and calculated as relative light units. NFkB-LUC, three NFkB binding sites upstream of luciferase cDNA. RLU, relative light unit.

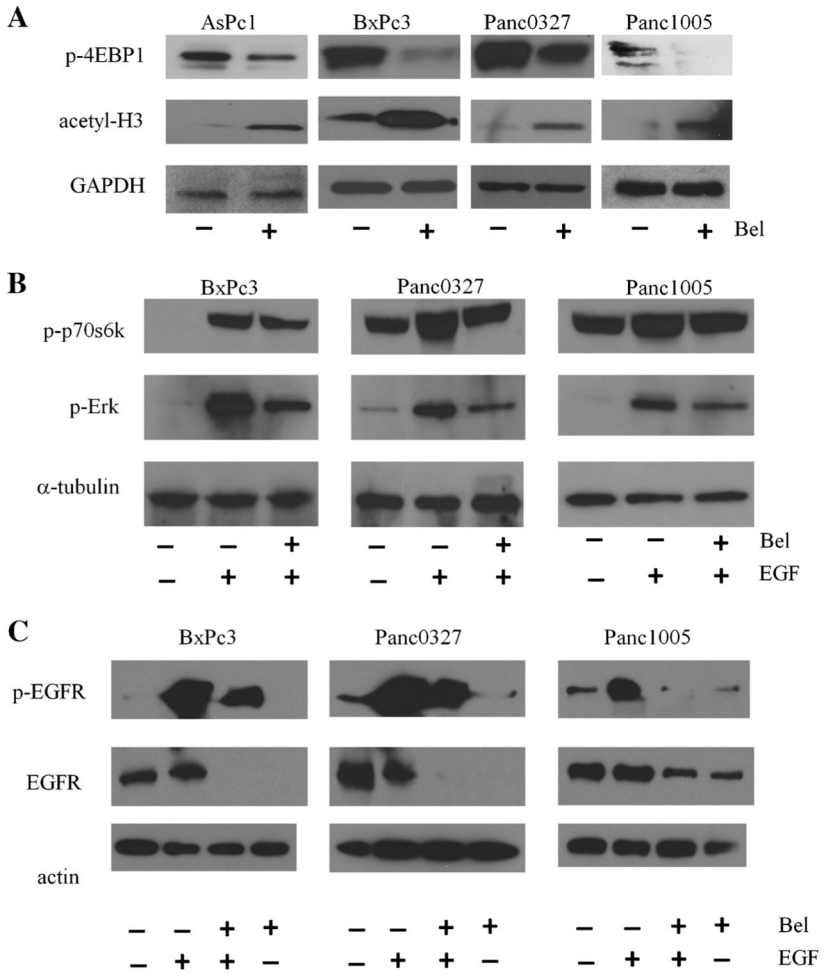


**Figure 4.**

Effect of belinostat on the expression levels of acetylated histone 3, phospho-4EBP1, -Erk, and -p70S6k. Panel (A): Western blots were probed with antibodies directed against acetyl-H3 (acetylated histone 3) and phospho-4EBP1. Cell lysates were prepared after 24 h treatment of pancreatic cancer cells with 1 μM belinostat. Panel (B): Western blot analysis for phospho-Erk, and phospho-p70S6k. Cells were serum-starved overnight, cultured with belinostat for 4 h before EGF (15 ng/mL) was added for an additional 5 min. Panel (C): Western blot analysis for phospho-EGFR and total EGFR. Following serum starvation overnight, cells were pretreated with 1 μM belinostat for 4 h and stimulated with EGF (15 ng/mL) for 5 min.

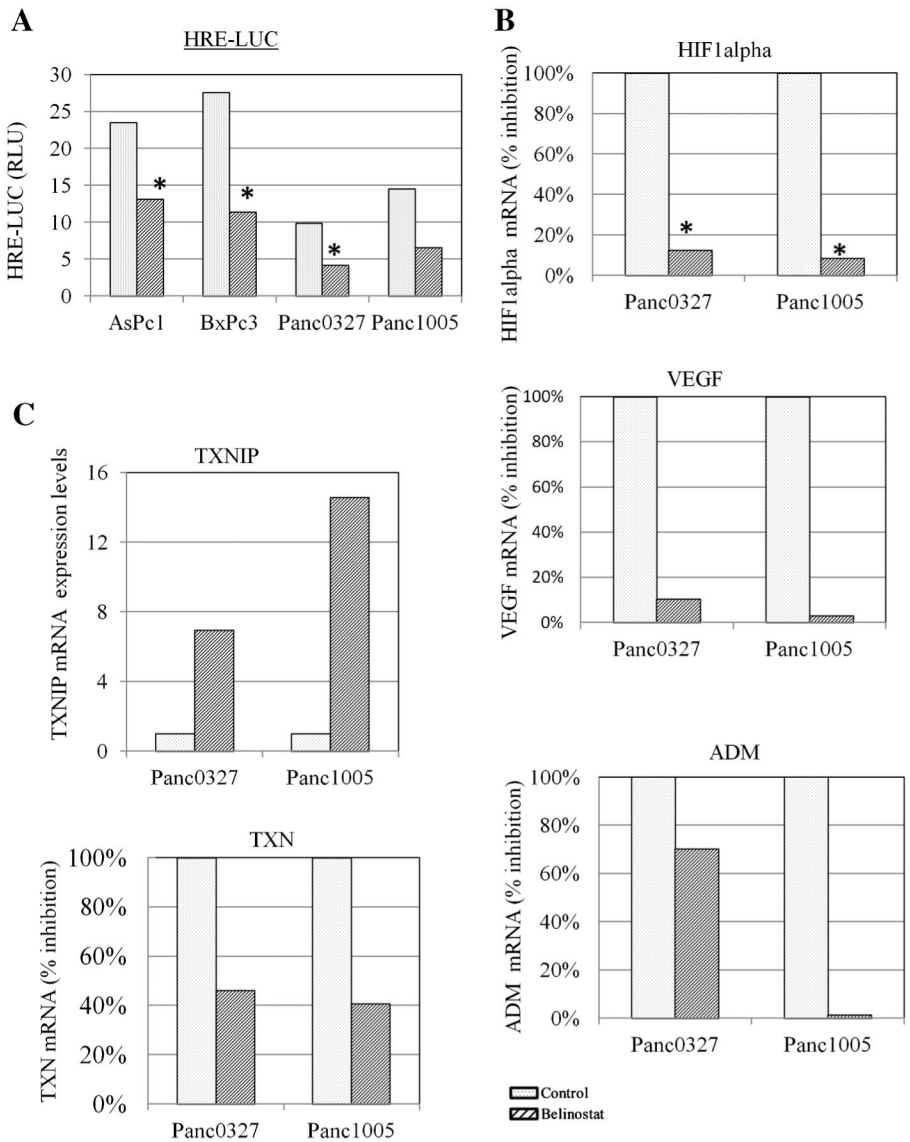


**Figure 5.**

Regulation of HIF signaling by belinostat. Panel (A): HRE reporter assay. Cells were transfected with *renilla* and a reporter construct containing hypoxia response element (HRE-LUC) and incubated for 24 h either with or without 1 μM belinosta. HRE reporter activity was normalized to *renilla* activity and calculated as relative light units (RLU). Panel (B): Real-time RT-PCR. Cells were treated with belinostat (1 μM, 24 h), and RNA was extracted for real-time RT-PCR for VEGF, HIF1α, and ADM. Gene expression levels were normalized to expression of GAPDH. Panel (C): Real time RT-PCR was performed to analyze expression levels of TXN and TXNIP.

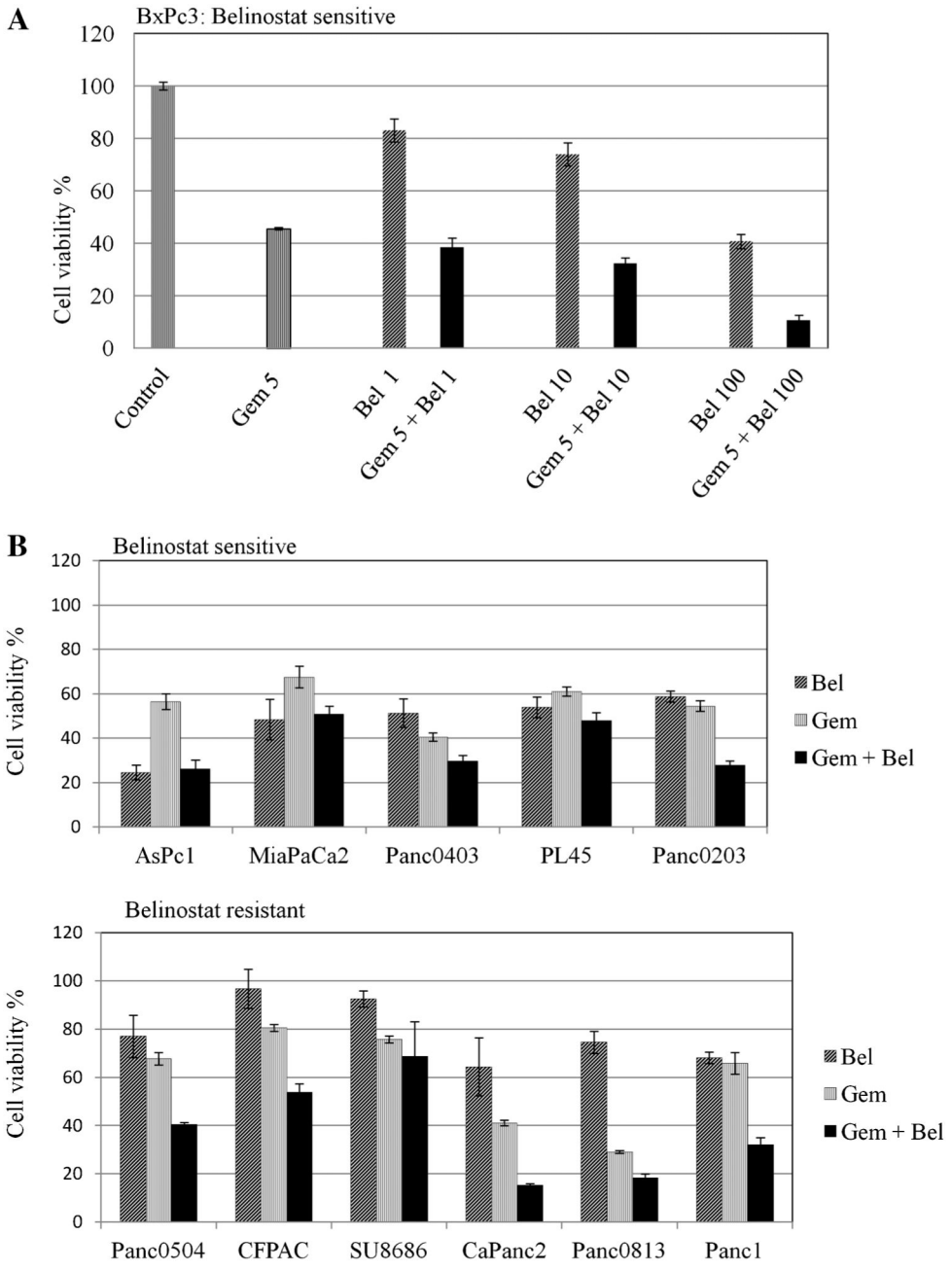

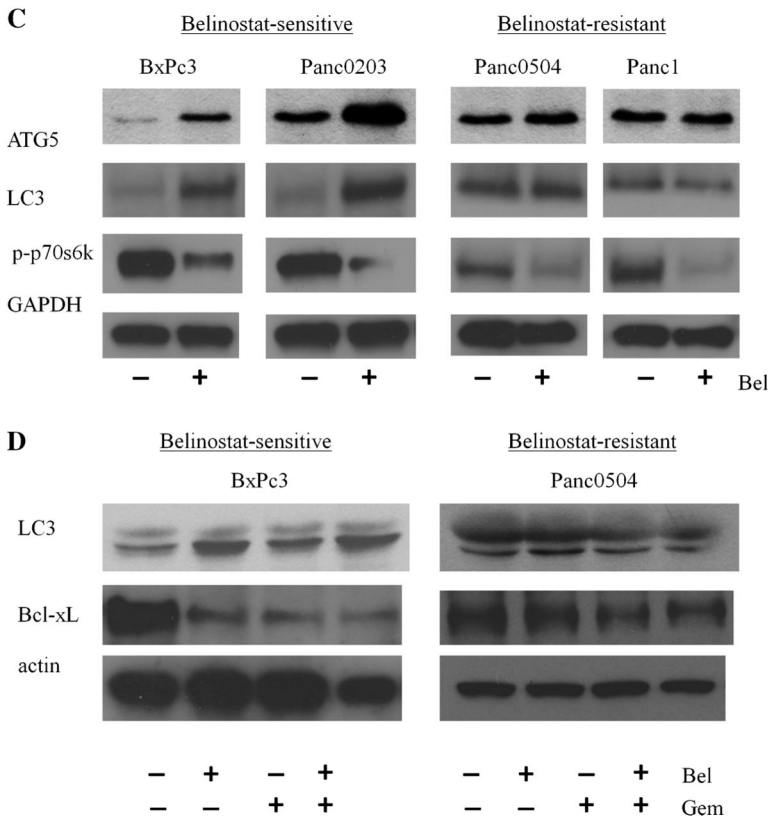


**Figure 6.**

Synergy between belinostat and gemcitabine in vitro. Panel (A) MTT assays. BxPc3 pancreatic cancer cells were cultured in 96-well plates and treated for 48 h with either gemcitabine, belinostat or the combination of both. MTT assay measured cell number relative to diluent control. A series of combination of gemcitabine and belinostat were tested. Gem 5: gemcitabine 5 μg/mL; Bel 1, 10, 100: belinostat 1, 10, 100 μM; Gem + Bel: combination of both drugs. Panel (B): Synergy between belinonstat and gemcitabine in both belinostat-sensitive and -resistant cell lines. One combination of gemcitabine and belinostat was tested. Gem, gemcitabine 5 ug/mL; Bel, belinostat 1 μM; Gem + Bel, combination of both drugs. Results represent the mean ± SD of two independent experiments with quadruplicates for each experimental and control group. Panel (C): Expression levels of ATG5, LC3, and phosphorylated p70s6k (p-p70s6k) from pancreatic cancer cell lines treated with 1 μM belinostat for 24 h were examined. Panel (D): Western blot analysis of the expression levels of LC3 and Bcl-xL were examined in cell lines treated with belinostat, gemcitabine, or the combination of both.

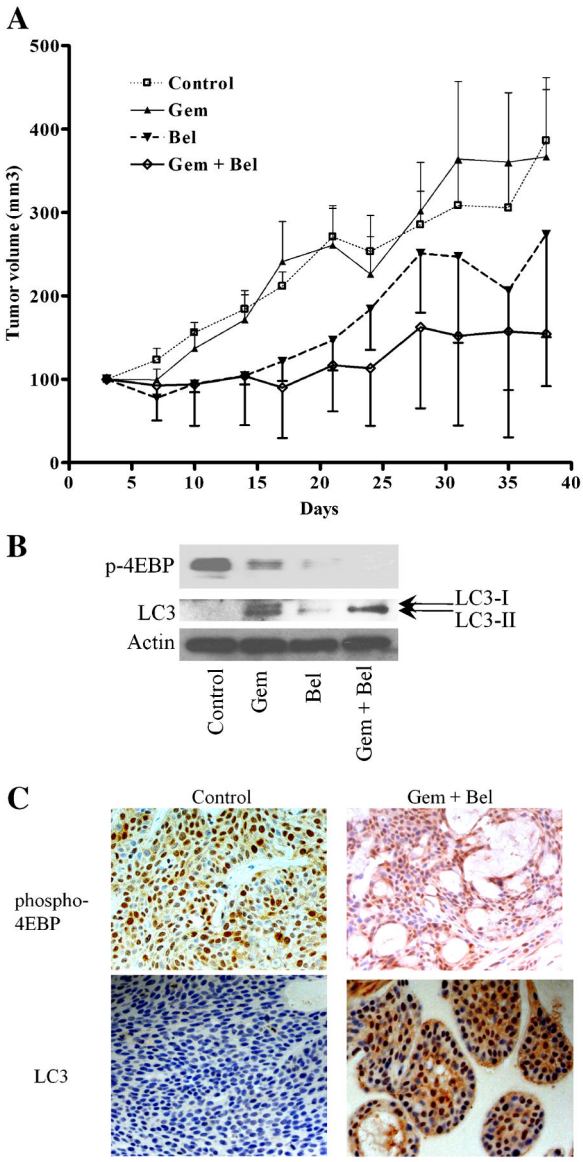


**Figure 7.**

Anti-proliferative activity of belinostat in animal models. Panel (A): Xenografts from four groups of six mice each were treated with either gemcitabine (15 mg/kg), belinostat (30 mg/kg) or the combination of both; and tumor size was monitored. Treatments were administered three times a week. Control treatment was diluent (100 mg/mL L-arginine in water). Tumors (two per mouse) were harvested from euthanized mice on day 38 and weighed. Tumors were divided in half. Panel (B): Western blot analysis of protein lysates prepared from tumor. Blots were probed with antibodies against phosphorylated 4EBP1 and LC3. Actin was used as loading control. Panel (C): Immunohistochemistry analysis of formalin fixed tumors against anti-phospho-4EBP1 and LC3. Bel, belinostat; Gem, gemcitabine; Gem + Bel, belinostat plus gemcitabine.

*Mol Carcinog*. Author manuscript; available in PMC 2014 September 01.

**Table 1**

Mouse Body Weights[#]

| | Control | | Gem | | Bel | | Gem + Bel | | |
|---|---|---|---|---|---|---|---|---|---|
| **Day** | **AVG** | **SD** | **AVG** | **SD** | **AVG** | **SD** | **AVG** | **SD** | ***t*-test[a]** |
| 3 | 100 | 0.0 | 100 | 0.0 | 100 | 0.0 | 100 | 0.0 | NS |
| 7 | 102 | 1.7 | 103 | 3.3 | 105 | 1.6 | 101 | 1.6 | NS |
| 10 | 104 | 5.9 | 101 | 3.4 | 103 | 2.8 | 100 | 1.7 | NS |
| 14 | 107 | 3.3 | 105 | 4.9 | 107 | 2.9 | 101 | 6.9 | NS |
| 17 | 110 | 4.2 | 107 | 4.9 | 109 | 3.5 | 104 | 1.3 | NS |
| 21 | 111 | 4.3 | 111 | 7.9 | 109 | 3.6 | 106 | 2.1 | NS |
| 24 | 110 | 3.8 | 111 | 5.3 | 109 | 3.3 | 108 | 1.7 | NS |
| 28 | 109 | 4.1 | 111 | 5.8 | 110 | 3.7 | 108 | 1.5 | NS |
| 31 | 107 | 5.1 | 112 | 6.4 | 109 | 3.9 | 107 | 2.0 | NS |
| 35 | 111 | 12.6 | 115 | 5.8 | 113 | 3.7 | 110 | 1.6 | NS |
| 38 | 110 | 5.4 | 116 | 5.9 | 115 | 3.5 | 110 | 1.8 | NS |
| 42 | 109 | 5.2 | 118 | 6.2 | 114 | 3.5 | 111 | 2.7 | NS |
| 45 | 111 | 4.2 | 119 | 7.5 | 113 | 2.6 | 112 | 2.5 | NS |

Gem, gemcitabine; Bel, belinostat; Gem + Bel, combination of gemcitabine and belinostat; AVG, average; SD, standard deviation.

[#]Weights in grams.

[a]*t*-test: significant difference by *t*-test; *P*-value (*, <0.05; **, <0.001); NS, not significant.

**Table 2**

Mouse Organ Weights[#]

| | Control | | Gem | | Bel | | Gem + Bel | | |
|---|---|---|---|---|---|---|---|---|---|
| | **AVG** | **SD** | **AVG** | **SD** | **AVG** | **SD** | **AVG** | **SD** | ***t*-test[a]** |
| Spleen[b] | 140.0 | 26.5 | 210.0 | 20.0 | 153.3 | 37.9 | 235.0 | 21.2 | ** |
| Kidney | 373.3 | 41.6 | 360.0 | 72.1 | 346.7 | 50.3 | 333.3 | 50.3 | NS |
| Liver | 1420.0 | 474.7 | 2046.7 | 362.0 | 1656.7 | 161.7 | 1723.3 | 153.7 | NS |

Gem, gemcitabine; Bel, belinostat; Gem + Bel, combination of gemcitabine and belinostat; AVG, average; SD, standard deviation.

[#]Weights in grams.

[a]*t*-test: significant difference by *t*-test; *P*-value (*, <0.05; *, <0.001); NS, not significant.

[b]Control < Gem** ($P = 0.0004$); control < Gem + Bel** ($P < 0.0001$).

**Table 3**

Complete Blood Count

| | Control | | Gem | | Bel | | Gem + Bel | | |
|---|---|---|---|---|---|---|---|---|---|
| **Cell ID** | **AVG** | **SD** | **AVG** | **SD** | **AVG** | **SD** | **AVG** | **SD** | ***t*-test[a]** |
| WBCs (K/μL) | 5.6 | 2.4 | 3.3 | 0.8 | 4.9 | 1.3 | 2.3 | 1.1 | NS |
| Neutrophills (K/μL) | 2.6 | 1.1 | 1.8 | 0.4 | 2.4 | 0.7 | 1.4 | 0.8 | NS |
| Lymphocytes (K/μL) | 2.9 | 1.3 | 1.3 | 0.2 | 2.2 | 0.8 | 0.8 | 0.3 | NS |
| Monocytes (K/μL) | 0.1 | 0.1 | 0.1 | 0.1 | 0.1 | 0.1 | 0.1 | 0.0 | NS |
| Eosinophils (K/μL) | 0.0 | 0.0 | 0.0 | 0.0 | 0.1 | 0.0 | 0.0 | 0.0 | NS |
| Basophils (K/μL) | 0.0 | 0.0 | 0.0 | 0.0 | 0.0 | 0.0 | 0.0 | 0.0 | NS |
| RBCs[b] (M/μL) | 7.5 | 0.4 | 6.2 | 0.9 | 8.0 | 0.4 | 5.8 | 0.1 | * |
| Hb[c] (g/dL) | 11.1 | 0.8 | 9.7 | 1.4 | 11.7 | 0.3 | 9.8 | 0.3 | ** |
| Platelets[d] (K/μL) | 723.0 | 314.1 | 590.0 | 37.0 | 861.0 | 69.2 | 1019.3 | 91.6 | * |

Gem, gemcitabine; Bel, belinostat; Gem + Bel, combination of gemcitabine and belinostat; AVG, average; SD, standard deviation.

[a] *t*-test: significant difference by *t*-test; *P*-value (*, <0.05; **, <0.001); NS, not significant.

[b] Bel > Gem + Bel*.

[c] Bel > Gem + Bel**.

[d] Gem < Gem + Bel*.

*Mol Carcinog*. Author manuscript; available in PMC 2014 September 01.

**Table 4**

Serum Chemistry

| | Control | | Gem only | | Bel only | | Gem + Bel | | |
|---|---|---|---|---|---|---|---|---|---|
| **Molecules ID** | **AVG** | **SD** | **AVG** | **SD** | **AVG** | **SD** | **AVG** | **SD** | ***t*-test[a]** |
| ALK PHOS | 90.0 | 8.5 | 67.7 | 30.6 | 80.7 | 8.4 | 68.0 | 14.7 | NS |
| GGT | 3.7 | 1.2 | 4.7 | 0.6 | 4.7 | 0.6 | 4.7 | 0.6 | NS |
| GOT (AST) | 84.0 | 14.8 | 227.3 | 112.3 | 125.3 | 21.5 | 157.3 | 78.2 | NS |
| GPT (ALT) | 32.0 | 6.6 | 51.3 | 16.0 | 48.7 | 23.8 | 58.3 | 38.1 | NS |
| AML | 105.7 | 104.0 | 302.7 | 205.4 | 686.7 | 430.3 | 854.3 | 529.6 | NS |
| BUN | 2.0 | 0.0 | 3.1 | 1.3 | 7.7 | 4.4 | 10.5 | 7.4 | NS |
| GLUCOSE | 17.0 | 8.2 | 46.7 | 24.8 | 84.7 | 65.2 | 84.5 | 88.7 | NS |
| PHOS | 1.9 | 0.0 | 1.9 | 0.0 | 3.8 | 2.4 | 5.2 | 2.9 | NS |
| CALCIUM | 5.0 | 0.0 | 5.0 | 0.0 | 6.5 | 2.5 | 7.9 | 2.6 | NS |
| ALB | 0.1 | 0.1 | 0.5 | 0.4 | 1.5 | 0.9 | 2.1 | 1.3 | NS |
| CHOLEST | 50.0 | 0.0 | 55.3 | 6.1 | 83.7 | 48.0 | 120.0 | 60.8 | NS |
| URIC | 1.5 | 0.5 | 1.6 | 0.1 | 1.5 | 0.3 | 1.7 | 0.4 | NS |
| CK | 289.7 | 38.8 | 1145.0 | 0.0 | 732.3 | 208.7 | 951.7 | 430.1 | NS |
| CREATIN | 0.3 | 0.1 | 0.2 | 0.1 | 0.3 | 0.1 | 0.3 | 0.1 | NS |
| TBIL | 0.1 | 0.0 | 0.1 | 0.0 | 0.1 | 0.0 | 0.1 | 0.0 | NS |
| T PROT | 4.7 | 1.3 | 4.4 | 0.9 | 5.2 | 0.3 | 4.3 | 0.4 | NS |
| GLOB | 5.6 | 0.0 | 4.2 | 0.1 | 3.8 | 0.9 | 2.2 | 1.4 | NS |

Gem, gemcitabine; Bel, belinostat; Gem + Bel, combination of gemcitabine and belinostat; AVG, average; SD, standard deviation; ALK PHOS, alkaline phosphatase; GGT, γ-glutamyl transpeptidase; GOT (AST), glutamate oxaloacetate transaminase, glutamate pyruvate transaminase, amylase, blood urea nitrogen, glucose levels (unstarved), phosphate, calcium, albumin, cholesterol, uric acid, creatine kinase, creatinine, total bilirubin, total protein, globulin.

[a] *t*-test: significant difference by *t*-test; *P*-value (*, <0.05; **, <0.001); NS, not significant.